$MgO–TiO_2$ mixed oxide nanoparticles: Comparison of flame synthesis versus aerogel method; characterization, and photocatalytic activities

Khadga M. Shrestha
Department of Chemistry, Kansas State University, Manhattan, Kansas 66506

Christopher M. Sorensen
Department of Physics, Kansas State University, Manhattan, Kansas 66506

Kenneth J. Klabunde[a)]
Department of Chemistry, Kansas State University, Manhattan, Kansas 66506

(Received 6 May 2012; accepted 16 August 2012)

Titanium dioxide (TiO_2) and mixed oxides, i.e., mixtures of magnesium oxide and titanium dioxide ($MgO–TiO_2$) with different ratios were synthesized by two methods—flame synthesis and aerogel, for comparison of their properties. The samples were characterized by powder x-ray diffraction (pXRD), energy-dispersive x-ray spectroscopy, Fourier transform infrared spectroscopy, Brunauer-Emmet-Teller method of surface area measurements, ultraviolet-visible spectroscopy (UV-vis), and transition electron microscopic analysis. The pXRD patterns of different mixed oxides with different mole ratios revealed that there were formations of different compositions and phases. These mixed oxides were also used as photocatalysts in the UV-vis light to oxidize acetaldehyde, and carbon dioxide (CO_2) was measured as a product. The mixed oxides with low content of MgO (~1–2 mol%) were found to be more UV-active photocatalysts for the degradation of acetaldehyde than the degradation by Degussa P25 and as-synthesized TiO_2, the highest by the $MgO–TiO_2$ mixed oxides of 1:50 ratio when comparisons were carried out among the samples prepared by the same method. Furthermore, the mixed oxides prepared by the aerogel method were found to be superior photocatalysts compared with the mixed oxides of equal ratio prepared by flame synthesis. This effect of insulator, MgO, on the photocatalytic activity of semiconductor, TiO_2, was found to be interesting and can be applied for other applications as environmentally friendly materials.

I. INTRODUCTION

Titanium dioxide (TiO_2), a semiconductor, is traditionally used in pigments, as photocatalyst, as a supporter of catalysts, and for water purification.[1–3] In the last two decades, TiO_2 nanomaterials with various morphologies—nanoparticles, nanotubes, nanorods—have been synthesized by various methods.[4–11] As the material is UV-active, the TiO_2 nanomaterials have been widely investigated as photocatalysts in the UV region[12–14]; the photocatalytic activities have been enhanced in visible and UV regions by doping with various metal- and nonmetal-based materials.[15–19]

MgO, an insulator, is traditionally used for the preparation of cement, medicines, insulators, desiccants, and optical materials.[20] In recent decades, people have given attention to the synthesis of MgO nanomaterials with different morphologies—nanoparticles, nanotubes, and nanorods—which have been investigated for different purposes[21–27]; MgO nanomaterials have been investigated as catalysts, adsorbents, and destructive adsorbents for toxins, including chemical warfare agents.[28–30]

There are many reports about the synthesis and properties of composite materials of TiO_2 with other oxides—TiO_2–silicon dioxide (SiO_2), TiO_2–cerium oxide (CeO_2), TiO_2–tin dioxide (SnO_2), TiO_2–zirconium oxide (ZrO_2), TiO_2–aluminum oxide (Al_2O_3), TiO_2–ferric oxide (Fe_2O_3), TiO_2–Ruthenium oxide (RuO_2), and TiO_2–iridium oxide (IrO_2)—in the form of nanomaterials.[31–43] Similarly, there are many reports about the mixed oxides of MgO with other oxides—$MgO–Al_2O_3$, $MgO–SnO_2$, $MgO–ZrO_2$, $MgO–CeO_2$, $MgO–SiO_2$, and MgO-samarium (III) oxide (Sm_2O_3)—and their properties.[44–56] However, there are relatively few reports about the synthesis of $MgO–TiO_2$ mixed oxides[57–61]; and there are no reports about the flame synthesis of $MgO–TiO_2$ mixed oxides to the best of our knowledge. Herein we report for the first time synthesis of $MgO–TiO_2$ mixed oxide nanoparticles by the flame synthesis. Our primary goal was to compare the properties of these mixed oxides obtained by aerogel versus flame synthesis (low temperature versus high temperature methods).

TiO_2 and MgO are environmentally friendly and economically low in cost, and pure TiO_2 and MgO nanomaterials have been widely investigated. However, their mixed system has rarely been investigated in either

[a)]Address all correspondence to this author.
e-mail: kenjk@ksu.edu
DOI: 10.1557/jmr.2012.288

photocatalytic or nonphotocatalytic reactions.[62–65] Furthermore, most of MgO–TiO_2 mixed oxides have been prepared by sol-gel methods in the presence of organic media. For an example, TiO_2 and MgO nanomaterials are usually prepared by the hydrolysis of their corresponding alkoxides in the presence of organic solvents like alcohol and toluene.

It is important to note that the flame synthesis method is continuous and economically more viable than the sol-gel method; so it might be worthwhile to synthesize most samples by this method. However, it is necessary to find out whether the mixed oxide samples prepared by flame synthesis have similar properties or not when compared with properties of similar samples prepared by the aerogel (sol-gel) method. Therefore, we synthesized the mixed oxide nanomaterials of MgO and TiO_2 with different ratios by both aerogel[66] and flame synthesis,[67] and compared their properties. To the best of our knowledge, this is the first time such comparison has been made based on experimentation.

We characterized the physical properties by different techniques and used them as photocatalysts for the mineralization of acetaldehyde (CH_3CHO), a common outdoor and indoor pollutant, using both UV and visible light. We found that these samples demonstrated enhanced photocatalytic activities over pure TiO_2 in UV light with low content of MgO; particularly the mixed oxides of MgO–TiO_2 (1:50 M ratio) prepared by both methods were found to be a superior composition for the photooxidation of CH_3CHO in UV light. Moreover, the photocatalytic activity of the MgO–TiO_2 prepared by the aerogel method was found to be better than that of the samples prepared by flame synthesis.

II. EXPERIMENTAL

A. Flame synthesis of TiO_2 and MgO–TiO_2 nanoparticles

TiO_2 nanoparticles were prepared by using titanium (IV) isopropoxide (Sigma-Aldrich, St. Louis, MO) as a Ti-precursor; the precursor was dissolved in methanol (Fisher Chemical, Pittsburgh, PA) in the presence of acetylacetone (Fisher Chemical). In a particular experiment, 3 mL of titanium (IV) isopropoxide was dissolved in a mixture of 5 mL methanol and 3 mL acetylacetone and stirred. Then the solution was used for the synthesis of TiO_2 during the flame synthesis.

The magnesium and titanium precursors were used to prepare MgO–TiO_2 mixed oxides with molar ratios of 2:1, 1:1, 1:2, 1:20, 1:50, and 1:100. For the synthesis of mixed oxides, titanium (IV) isopropoxide was dissolved in methanol in the presence of acetylacetone; acetylacetone slows the hydrolysis of the titanium precursor. Magnesium acetate was dissolved in methanol. In a particular experiment, 3 mL titanium (IV) isopropoxide was dissolved in 3 mL acetylacetone and 2.1 g of hydrated magnesium acetate (Alfa-Aesar, Ward Hill, MA) was dissolved in 5 mL methanol. These two solutions were mixed together and stirred from which 1:1 M ratio of MgO and TiO_2 could be prepared. Then the mixed solution was injected into the glass tube and converted into mist with the help of an ultrasonic nebulizer fixed at the bottom of the tube which was extracted from an ultrasonic humidifier (Model V5100 NS; PN 32GB5100B09; Kaz, Inc., Southborough, MA); the mist along with the flow of ultra high pure (UHP) nitrogen (rate = 2 L/min) was driven to the flame of a burner. The flame of the burner was prepared by passing industrial oxygen (10 L/min) and methane (4 L/min) gases (Linweld, Sioux City, IA). We did not measure the flame temperature during the experiment. The reported flame temperature produced by a mixture of 80% methane and 20% oxygen is 1974 °C[68]; the temperature could be increased from 1601 to 2692 °C with increase in percentage of oxygen,[69] and the adiabatic flame temperature in the hottest region was about 2781 °C.[70] Since sufficient oxygen was passed during our experiment, to burn all combustible materials so as to produce metal oxide particles from metal precursors, possibly the flame temperature at the hottest zone was expected around 2700 °C.

The outer cold surface of a steel bowl with a flat bottom containing ice water was set at the height of 10 cm above the nozzle of the burner so as to collect a deposit of the oxide samples by the thermophoresis process. The precursor was passed through the burner for about 30 min. Then, the oxide sample was scrapped out and collected.

B. Synthesis of MgO–TiO_2 mixed oxide by aerogel method

Mixed oxides of MgO and TiO_2 were also prepared by the aerogel method with the same molar ratios as those prepared by the flame synthesis. For the synthesis of the mixed oxides, the desired amount of clean magnesium ribbon (Sigma-Aldrich) was allowed to react with methanol completely, to obtain a magnesium methoxide suspension in methanol.[66] Then the magnesium methoxide suspension and titanium (IV) isopropoxide in toluene were mixed together, and stirred with a magnetic stirrer. A stoichiometric amount of water was added to the mixed suspension for the complete hydrolysis of both metal alkoxides with continuous stirring so as to form a gel; the ratio of methanol to toluene was 2:3 as an appropriate mixture of methanol and toluene that could help to form the gel rapidly. The gel was treated for supercritical drying followed by calcination. In a particular experiment, 0.8 g of clean Mg ribbon was allowed to react with 40 mL methanol so as to form magnesium methoxide. Ten milliliters of titanium (IV) isopropoxide was dissolved in 60 mL toluene; both of them were mixed together and stirred to get a 1:1 M ratio of MgO and TiO_2. Then 3.5 mL of water with two

drops of 11.5 N HCl was added for the complete hydrolysis of both metal alkoxides, and a gel was formed. After 4 h of aging, the gel was transferred to an autoclave and heated at 265 °C to attain a supercritical condition for subsequent venting of solvent. The solid aerogel obtained was then calcined at 500 °C in air for 1 h with heating and cooling at the rate of 5 °C/min.

C. Characterization

1. Powder x-ray diffraction (pXRD)

The samples prepared by both flame synthesis and aerogel method were characterized by the pXRD patterns with 2θ angle in the range of 20–80° measured with a Scintag, Inc. XDS 2000 spectrometer (Cupertino, CA); the x-ray was Cu K_α radiation with applied voltage of 40 kV and the current ~40 mA.

2. Transmission electron microscopy (TEM) and scanning electron microscopy (SEM)

The sizes and morphologies of these metal oxide nanomaterials were observed by TEM, and the elemental analyses were carried out by SEM. SEM experiments were carried out by using a Scanning Electron Microscope-S3500N, Hitachi Science System, Ltd., Tokyo, Japan, at the Entomology Department of Kansas State University (KSU), microscopy and imaging facility. TEM experiments were carried out by using a transmission electron microscope, Phillips 100 (Eindhoven, The Netherlands) at the Biology department of KSU.

3. Brunauer-Emmett-Teller (BET) method

Specific surface areas and pore diameters of TiO_2 and $MgO–TiO_2$ nanoparticles were measured by the BET method. The measurements were carried out using Microsorb II 2300 and Quantachrome NOVA 1200 instrumentation (Boynton Beach, FL) at 77 K using liquid nitrogen.

4. UV-vis and Fourier transform infrared (FTIR) analysis

A Cary 500 UV-vis-NIR spectrometer (Aligent Technologies, Santa Clara, CA) with reflectance accessory was used in the range of 200–800 nm. The sample cell was made of two transparent calcium fluoride discs, a Teflon O-ring and screw type combination in which the oxide materials were packed between two discs and the O-ring. In this technique, absorption of a solid material was measured by using diffuse reflectance mode; the instrumental system calculates the absorption automatically measuring the diffuse reflectance.[71] Polytetrafluoroethylene (PTFE) powder of ~100 μm particle size (Sigma-Aldrich) was taken as a reference material. After using the reference sample, absorption of individual oxide sample was measured. Furthermore, some samples were characterized by FTIR using Thermo Necolet Nexus 670 FTIR (Aligent Technologies, Santa Clara, CA) with Avatar Diffuse Reflectance accessory.

5. Photocatalytic study

The photocatalytic oxidation of acetaldehyde was carried out with aerial oxygen in a 305 mL static cylindrical glass reactor with a water-jacketed base at room temperature. During the experiment, a catalyst was placed in a circular glass dish (radius = 7 mm) mounted in the reactor with a small magnetic stirrer underneath the dish. Then side tubes of the reactor were closed with rubber septa; 100 μL of liquid acetaldehyde (Sigma-Aldrich) was introduced and then the opening of the reactor was closed immediately with the quartz window. The acetaldehyde (boiling point = 25 °C) was converted to vapor at room temperature; the mixture of acetaldehyde and air was stirred for 40 min in the dark for achieving equilibrium of the reacting molecules prior to illumination. Then 35 μL of gas from the reactor was extracted periodically with a syringe through a septum and the gas was injected into the gas chromatography - mass spectrometry (GC-MS) port (Shimadzu GCMS-QP 5000, Kyoto, Japan); the temperatures of the injector, column, and detector were maintained at 40, 200, and 280 °C, respectively. After the injection of the third sample from the reactor at 40 min, UV light ($\lambda > 320$ nm) was introduced through the quartz glass from the 1000 W high-pressure xenon lamp (Oriel Instrument, Stratford, CT, Model 66921) at the height of 20 cm.

III. RESULTS AND DISCUSSION

A. X-ray analysis

The pXRD patterns of $MgO–TiO_2$ mixed oxides with relatively high content of MgO—2:1, 1:1, and 1:2 M ratios of MgO and TiO_2—demonstrated the formation of titanates of Mg with different chemical compositions: $MgTiO_3$, Mg_2TiO_4 and $MgTi_2O_5$. The pXRD patterns of the $MgO–TiO_2$ mixed oxides with 2:1 ratio prepared by both aerogel and flame synthesis demonstrated the formation of $MgTi_2O_4$ [Figs. S1(a) and S1(b) where "S" stands for supporting information]; however, the mixed oxide prepared by the flame synthesis was found to be relatively more crystalline than that prepared by aerogel method. The pXRD pattern of the $MgO–TiO_2$ mixed oxides with 1:1 M ratio prepared by the flame synthesis showed the formation of two compounds: $MgTi_2O_4$ as a major product and $MgTiO_3$ as the minor product [Fig. S2(a)]. The pXRD patterns of the mixed oxides with M ratio of 1:1 prepared by aerogel demonstrated the formation of $MgTi_2O_5$ [Fig. S2(b)]. The pXRD pattern of the mixed

oxides with ratio of 1:2 prepared by the flame synthesis demonstrated the formation of $MgTiO_3$ as the major product and TiO_2 (anatase and rutile) as the minor product [Fig. S3(a)]. The pXRD patterns of mixed oxides with ratio 1:2 prepared by aerogel method demonstrated the formation of $MgTi_2O_5$ but with a nearly amorphous nature [Fig. S3(b)].

Figures 1(a) and 1(b) show the pXRD patterns for the TiO_2 and the MgO–TiO_2 mixed oxides with ratios 1:20, 1:50, and 1:100. TiO_2 prepared by flame synthesis process were found to be in both anatase and rutile phases [Fig. 1(a)]; the ratio of anatase and rutile was found to be about one. However, TiO_2 aerogel was found to be only in the anatase phase [Fig. 1(b)]. This could be possible as the anatase phase usually forms at lower temperature (<500 °C); the rutile phase and anatase phases form at relatively higher temperature (>500 °C).[72] Herein aerogel samples were calcined at relatively low temperature (500 °C) and the samples from the flame synthesis were prepared at higher temperature (cal. >500 °C). The MgO–TiO_2 mixed oxides with 1:20, 1:50, and 1:100 ratios prepared by flame synthesis showed the presence of both anatase and rutile TiO_2 and the aerogel samples with these ratios showed the presence of anatase only. However, the pXRD patterns of MgO–TiO_2 (1:20, 1:50, and 1:100) mixed oxides prepared by both methods did not show the presence of MgO. The reason might be the low quantity of MgO and it could be well dispersed throughout the TiO_2. However, the presence of a small amount of Mg on the surface of mixed oxides was confirmed by energy-dispersive x-ray spectroscopic (EDX) analysis (Fig. S4). In MgO–TiO_2 mixed oxides with mole ratios of 1:50 and 1:100, the mole percentages of Mg were found to be ~1.9 and 1 respectively in total mole of Mg and Ti in the mixed oxides when prepared by aerogel method; similarly, the mole percentages of Mg were found to be ~1.1 and 0.4 in total mole of Mg and Ti in MgO–TiO_2 mixed oxides with mole ratios of 1:50 and 1:100 respectively when prepared by flame synthesis.

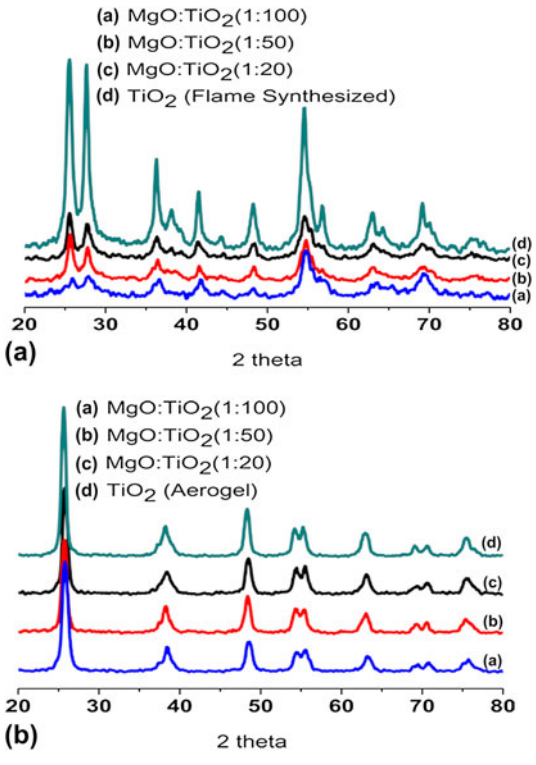

FIG. 1. pXRD patterns of MgO–TiO_2 with mol ratios of 1:100, 1:50, 1:20, and TiO_2 prepared by (a) flame synthesis (b) aerogel method.

B. Infrared analysis

TiO_2 and some MgO–TiO_2 (1:1 and 1:50) mixed oxides prepared by both flame synthesis and aerogel method were characterized by FTIR spectra (Figs. S5 and S6). The spectra of MgO–TiO_2 (1:1) mixed oxides were found to be different from the spectra of TiO_2 and MgO–TiO_2 (1:50); the spectra of MgO–TiO_2 (1:1) prepared by both flame and aerogel methods showed characteristic peaks below 500 cm^{-1} due to the rotational mode by IR absorption of Mg–O–Ti indicating the formation of titanates of Mg.[65] However, there were no characteristic peaks in this region for the pure TiO_2 and MgO–TiO_2 (1:50) mixed oxides.

C. BET data analysis

The samples were characterized with BET nitrogen (N_2) adsorption and desorption experiments; the specific surface area and pore diameter values of TiO_2 and the mixed oxides prepared by aerogel and flame synthesis are shown in Table I. The surface area of TiO_2 nanoparticles prepared by the flame synthesis process was found to be 98 m^2/g and the value was found to be 96 m^2/g when prepared by the aerogel method. Different specific surface area values were found for the mixed oxides of MgO and TiO_2 with various ratios prepared by both aerogel and flame synthesis. The surface areas were found to be greater for the MgO–TiO_2 mixed oxides in the form of titanates of Mg with ratios of 2:1, 1:1, and 1:2. The surface areas of the mixed oxides with these ratios prepared by aerogel

TABLE I. BET data for TiO_2 and MgO–TiO_2 samples prepared by flame synthesis and aerogel method calcined at 500 °C.

Samples prepared by flame synthesis	Surface area (m^2/g)	Pore diameter (nm)	Samples prepared by aerogel	Surface area (m^2/g)	Pore diameter (nm)
TiO_2	98	27	TiO_2	96	17
MgO–TiO_2 (2:1)	121	34	MgO–TiO_2 (2:1)	230	8
MgO–TiO_2 (1:1)	156	30	MgO–TiO_2 (1:1)	220	8
MgO–TiO_2 (1:2)	101	31	MgO–TiO_2 (1:2)	201	8
MgO–TiO_2 (1:20)	91	27	MgO–TiO_2 (1:20)	86	28
MgO–TiO_2 (1:50)	105	15	MgO–TiO_2 (1:50)	84	29
MgO–TiO_2 (1:100)	72	16	MgO–TiO_2 (1:100)	80	29

were found to be relatively greater than those prepared by flame synthesis. Higher values of the surface areas may be possibly due to the lower temperature for the synthesis in the aerogel method, which would minimize sintering. The surface areas of the mixed oxides with the low amount of MgO were found to be less than that of pure TiO_2 nanoparticles when prepared by both methods. These mixed oxides were found to be porous, especially mesoporous as pore diameters of the samples were in the range of 8–34 nm (Table I).

D. TEM analysis

Some mixed oxides were characterized by TEM analysis. Figure 2(a) shows TEM image of MgO–TiO_2 mixed oxides with ratio of 1:50 prepared by the flame synthesis process; the size of individual particles was in the range of 11–15 nm; the particle size is close to crystallite size of 12 nm calculated from the Scherrer's equation. The mixed oxide with 1:50 ratio prepared by aerogel method was also characterized by TEM [Fig. 2(b)]; the figure shows the particle size of ~10–20 nm; the particle size is close the crystallite size of 13 nm calculated from Scherrer's equation.

E. UV-vis absorption spectra

Samples were also characterized by UV-vis absorption spectra, and compared with the spectrum of Degussa P25 [Figs. 3(a) and 3(b)]. In the UV-vis spectra, the absorption by MgO–TiO_2 mixed oxides with high content of MgO (MgO:TiO_2 = 1:1 and 1:2) was found to be in the shorter wave length region due to the formation of titanates of Mg with different compositions. The spectra of as-prepared TiO_2 and the mixed oxides with low content of MgO were found to be slightly red-shifted. The band gap of pure TiO_2 and mixed oxides of MgO–TiO_2 (1:20, 1:50, and 1:100) prepared by aerogel method, which showed anatase phase of TiO_2 only from pXRD analysis, was found to be ~3.1 eV; the band gap of those types of samples prepared by flame synthesis, which showed both anatase and rutile phases of TiO_2, was found to be 2.9 eV. The absorption at longer wave length, red shift, possibly might be due to the various types of crystal defects. Furthermore, there were relatively stronger absorptions of UV light ($\lambda \geq 320$ nm) by the TiO_2 and mixed oxides prepared by the aerogel method, when compared with spectra of similar samples prepared by flame synthesis.

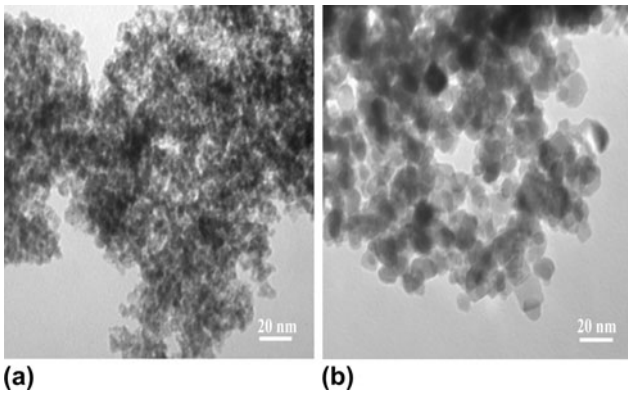

FIG. 2. TEM images of MgO–TiO_2 (1:50) samples prepared by (a) flame synthesis (b) aerogel method.

F. Photocatalysis studies

Samples prepared by both flame synthesis and aerogel method were used as photocatalysts using UV light. The oxidation of acetaldehyde in presence of air was studied at room temperature, 25 °C, and CO_2 was measured as a final product by the reaction: $2CH_3CHO + 5O_2 \rightarrow 4CO_2 + 4H_2O$. The CO_2 that accumulated inside the closed reactor was measured at different intervals [Figs. 4(a) and 4(b)]. No CO_2 was found to be formed in the dark or under visible light. Furthermore, UV-light was also introduced to the reactor containing acetaldehyde without oxide samples;

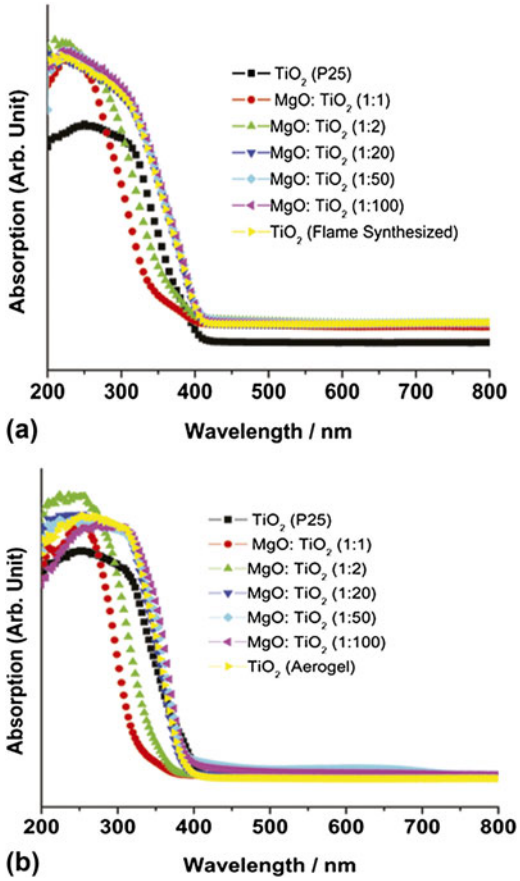

FIG. 3. UV-vis absorption spectra of Degussa P25, TiO_2 (as-synthesized), and MgO–TiO_2 mixed oxides with mol ratios of 1:1, 1:2, 1:20, 1:50, and 1:100 synthesized by (a) flame synthesis (b) aerogel method.

no CO_2 was found to be formed, indicating that oxide samples are indeed, photocatalysts.

The photocatalytic activities of the mixed oxides with different ratios and TiO_2 prepared by the same method were compared. The photocatalytic activities of MgO–TiO_2 (1:1) were found to be the lowest, and also note that these were the samples that absorbed only the shorter UV wave length and therefore, would probably absorb fewer photons overall at longer wave length of UV for the photocatalytic reaction.

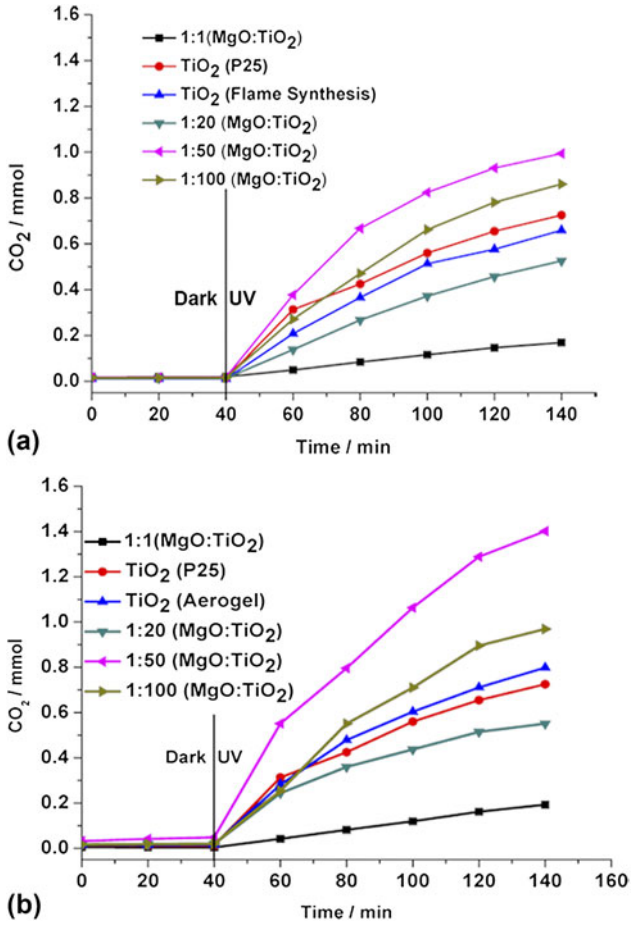

FIG. 4. Measurement of CO_2 produced from photocatalytic oxidation of acetaldehyde under UV light by Degussa P25, TiO_2 (as-synthesized), and MgO–TiO_2 mixed oxides with ratios of 1:1, 1:20, 1:50, and 1:100 as photocatalysts prepared by (a) flame synthesis (b) aerogel method.

When the amount of MgO was decreased in the mixed oxides, the catalytic activities were found to be enhanced. Interestingly, a maximum activity was obtained when MgO–TiO_2 with the ratio of 1:50 was used. Thus, small amounts of MgO were beneficial, for both flame-synthesized and aerogel samples. It should also be noted that aerogel samples were generally better photocatalysts than the flame-produced samples. The overall photocatalytic reactivity order for the oxide samples prepared by the flame synthesis process was found to be MgO–TiO_2 (1:50) > MgO–TiO_2 (1:100) > TiO_2 (Degussa P25) > TiO_2 (as-synthesized) > MgO–TiO_2 (1:20) > MgO–TiO_2 (1:1). The order for the aerogel samples was found to be MgO–TiO_2 (1:50) > MgO–TiO_2 (1:100) > TiO_2 (as-synthesized) > TiO_2 (Degussa P25) > MgO–TiO_2 (1:20) > MgO–TiO_2 (1:1). Slightly higher surface area could partially explain these trends, but the 1:50 ratio samples appeared to be special, and in particular the aerogel system. Indeed, the photocatalytic activities in UV light were found to be greater by the samples prepared by aerogel in every case (Table II).

When MgO is mixed with the TiO_2, there might be surface modification with change in surface energy. If a large amount of MgO, an insulator, is mixed, there would be more MgO on the surface, which would reduce TiO_2 surface. Furthermore, the mixed oxides with high content of MgO in the MgO–TiO_2 mixed oxides (2:1, 1:1, and 1:2) would form titanates of Mg that have high band gap; these compounds absorb at shorter wave length and are not favorable for the photocatalytic oxidation of acetaldehyde.

When a small amount of MgO is introduced to TiO_2, there must be good dispersion of MgO without formation of a separate crystalline phase of MgO. This might be the reason why there were no pXRD patterns of MgO in MgO–TiO_2 mixed oxides with ratios of 1:20, 1:50, and 1:100 although Mg was detected by EDX. The surface modification of the mixed oxide by the introduction of a small amount of MgO might produce different kinds of crystal defects on TiO_2. The crystalline structure of MgO might be also an important factor in developing more defects. MgO is coordinated octahedrally with coordination number 6 and {100} facets are predominant in the MgO microcrystalline structure.[73–75] At the surface of the mixed oxide, there might be a greater number of unsaturated sites of MgO so as to produce more defects in the mixed oxide. Furthermore, some Mg^{2+} could substitute

TABLE II. Comparison of amount of CO_2 produced by TiO_2 and MgO–TiO_2 mixed oxides with similar composition prepared by flame synthesis and aerogel method at the end of 140 min.[a]

	CO_2 (mmol) produced by				
Sample preparation methods	TiO_2	MgO:TiO_2 (1:1)	MgO:TiO_2 (1:20)	MgO:TiO_2 (1:50)	MgO:TiO_2 (1:100)
Flame synthesis	0.66	0.17	0.53	0.99	0.86
Aerogel	0.80	0.19	0.55	1.30	0.97

[a]UV light was introduced after 40 min in dark.

Ti^{4+} so as to produce crystal defects in TiO_2 crystals and cation vacancies (F-centers). Furthermore, there might be anion vacancies (V-centers) as the defects. These defects are probably important for the photocatalytic oxidation of acetaldehyde. F-centers could be both neutral or charged; the F-centers with charge have a tendency to trap electrons generated from photoexcitation, possibly leading to a separation of the hole-electron pair and suppress recombination; as a result, there would be an enhancement of the photocatalytic degradation of acetaldehyde.[76,77] Due to these defects, the MgO–TiO_2 with ratios of 1:50 and 1:100 absorbed at longer wave length than Degussa P25. The small amount of doped MgO might have created intermediate energy levels between the valence band and conductance band of TiO_2 so as to absorb at longer wave length. MgO–TiO_2 (1:50), ~2 mol% MgO, was found to be optimum for the photooxidation of acetaldehyde; the result is close to the reported data for the maximum oxidation of chlorophenol by 3% MgO-doped TiO_2 synthesized by the sol-gel method.[63] Larger (5%) or smaller (1%) loadings were not so effective.

As mentioned above, the aerogel samples were found to be superior to that of samples prepared by the flame synthesis when compared for equal ratio of mixed oxides. The Mg doped in the mixed oxide was found to be homogeneously distributed on the surface of mixed oxide particles when prepared by aerogel method, as indicated by EDX data, but this was not the case of mixed oxides prepared by flame synthesis. Furthermore, there were formations of both anatase and rutile phases of TiO_2 present in the mixed oxides with lower content of MgO on the surface of nanoparticles when synthesized by the flame synthesis. However, only the anatase phase was found to be formed when synthesized by the aerogel method.

It has been reported that the anatase phase is superior for the photocatalytic oxidation of organic compounds especially by the small porous anatase particles; the anatase TiO_2 might adsorb relatively more water and form hydroxyl group so as to enhance the degradation of acetaldehyde[63,78,79]; Ohno et al. revealed that relatively bigger rutile particles (>1 μm) with {110} and {110} faces were found to be active for the photocatalytic oxidation of water, an inorganic compound, using a suitable electron acceptor, whereas they found that smaller anatase particles were found to be very active for the oxidation of alcohols especially at low concentration. Smith and Ford demonstrated that more heat of oxygen adsorption was produced by anatase than produced by rutile[75]; in other words, more oxygen could be adsorbed on the surface of anatase leading to photocatalytic oxidation of acetaldehyde effectively. So the formation of anatase only in as-synthesized TiO_2 and in the MgO–TiO_2 mixed oxides of 1:20, 1:50, and 1:100 ratios prepared by aerogel played an important role for enhancing photocatalytic oxidation of acetaldehyde.

IV. CONCLUSIONS

The mixed oxides of MgO and TiO_2 with various ratios were prepared by flame synthesis and aerogel methods. From the pXRD patterns, titanates of MgO with different compositions were found to be formed using a relatively high content of MgO in the mixed oxides. When MgO content was relatively low, only the patterns of TiO_2 were found, indicating well-dispersed MgO; only the TiO_2 anatase phase was found in the aerogel samples, but both anatase and rutile were found in the mixed oxides prepared by flame synthesis. However, the presence of Mg could also be detected by EDX analysis. From the UV-vis spectra, it was found that the mixed oxide samples with low content of MgO absorbed at slightly longer wave length when compared with the spectrum of Degussa P25. These mixed oxides with low content of MgO were found to be more UV-active photocatalysts than TiO_2 for the mineralization of acetaldehyde. The MgO–TiO_2 mixed oxide with 1:50 ratio showed the highest photocatalytic degradation of acetaldehyde. When the photocatalytic activities of mixed oxides with equal ratio prepared by flame synthesis and aerogel method were compared, in each case an aerogel sample was found to be superior.

ACKNOWLEDGMENTS

The partial financial support of the Department of Energy (DF-FGO2-10ER16202) and KSU Targeted Excellence are acknowledged with gratitude.

REFERENCES

1. A.E. Jacobsen: Titanium dioxide pigments. *Ind. Eng. Chem.* **41**, 523 (1949).
2. E. Pramauro, M. Vincenti, V. Augugliaro, and L. Palmisano: Photocatalytic degradation of monuron in aqueous TiO_2 dispersions. *Environ. Sci. Technol.* **27**, 1790 (1993).
3. Y. Zhang, J.C. Crittenden, D.W. Hand, and D.L. Perram: Fixed-bed photocatalysts for solar decontamination of water. *Environ. Sci. Technol.* **28**, 435 (1994).
4. J. Liu, Y. Hu, F. Gu, and C. Li: Flame synthesis of ball-in-shell structured TiO_2 nanospheres. *Ind. Eng. Chem. Res.* **48**, 735 (2009).
5. K.T. Lim, H.S. Hwang, W. Ryoo, and K.P. Johnston: Synthesis of TiO_2 nanoparticles utilizing hydrated reverse micelles in CO_2. *Langmuir* **20**, 2466 (2004).
6. S.M. Liu, L.M. Gan, L.H. Liu, W.D. Zhang, and H.C. Zeng: Synthesis of single-crystalline TiO_2 nanotubes. *Chem. Mater.* **14**, 1391 (2002).
7. M. Zhang, Y. Bando, and K. Wada: Sol-gel template preparation of TiO_2 nanotubes and nanorods. *J. Mater. Sci. Lett.* **20**, 167 (2001).
8. C.A. Grimes: Synthesis and application of highly ordered arrays of TiO_2 nanotubes. *J. Mater. Chem.* **17**, 1451 (2007).
9. H. Yin, Y. Wada, T. Kitamura, S. Kambe, S. Murasawa, H. Mori, T. Sakata, and S. Yanagida: Hydrothermal synthesis of nanosized anatase and rutile TiO_2 using amorphous phase TiO_2. *J. Mater. Chem.* **11**, 1694 (2001).

10. A.V. Murugan, V. Samuel, and V. Ravi: Synthesis of nanocrystalline anatase TiO_2 by microwave hydrothermal method. *Mater. Lett.* **60**, 479 (2006).
11. A. Goossens, E.L. Maloney, and J. Schoonman: Gas-phase synthesis of nanostructured anatase TiO_2. *Chem. Vap. Deposition* **4**, 109 (1998).
12. T. Ohno, K. Takieda, S. Higashida, and M. Matsumura: Synergism between rutile and anatase TiO_2 particles in photocatalytic oxidation of naphthalene. *Appl. Catal., A* **244**, 383 (2003).
13. T. Kawahara, Y. Konishi, H. Tada, N. Tohge, J. Nishii, and S. Ito: A patterned TiO_2 (anatase)/TiO_2 (rutile) bilayer-type photocatalyst: Effect of the anatase/rutile junction on the photocatalytic activity. *Angew. Chem. Int. Ed.* **114**, 2935 (2002).
14. T. Ohno, K. Surukawa, and M. Matsumura: Photocatalytic activities of pure rutile particles isolated from TiO_2 powder by dissolving the anatase component in HF solution. *J. Phys. Chem. B* **105**, 2417 (2001).
15. Q. Sun and Y. Xu: Evaluating intrinsic photocatalytic activities of anatase and rutile TiO_2 for organic degradation in water. *J. Phys. Chem. C* **114**, 18911(2010).
16. T. Ohno, K. Sarukawa, and M. Matsumura: Crystal faces of rutile and anatase TiO_2 particles and their roles in photocatalytic reaction. *New J. Chem.* **26**, 1167 (2002).
17. O.K. Varghese, M. Paulose, T.J. LaTempa, and C.A. Grimes: High-rate solar photocatalytic conversion of CO_2 and water vapor to hydrocarbon fuels. *Nano Lett.* **9**, 731 (2009).
18. D.B. Hamal and K.J. Klabunde: Synthesis, characterization, and visible light activity of new nanoparticle photocatalysts based on silver, carbon, and sulfur-doped TiO_2. *J. Colloid Interface Sci.* **311**, 514 (2007).
19. A.D. Paola, E.G. Lopez, S. Ikeda, G. Marci, B. Ohtani, and L. Palmisano: Photocatalytic degradation of organic compounds in aqueous systems by transition metal-doped polycrystalline TiO_2. *Catal. Today* **75**, 87 (2002).
20. J.C. Bailor, H.J. Emeléus , R. Nyholm, and A.F. Trotman-Dikenson: *Comprehensive Inorganic Chemistry*, 1st ed. (Compendium Publishers, Elmsford, NY, **1**, 1973).
21. J. Zhan, Y. Bando, J. Hu, and D. Golberg: Bulk synthesis of single-crystalline magnesium oxide nanotubes. *Inorg. Chem.* **43**, 2462 (2004).
22. R. Richards, R.S. Mulukutla, I. Mishakov, V. Chesnokov, A. Volodin, V. Zaikovski, N. Sun, and K.J. Klabunde: Nanocrystalline ultrahigh surface area magnesium oxide as a selective base catalyst. *Scr. Mater.* **44**, 1663–1666 (2001).
23. R.M. Narske, K.J. Klabunde, and S. Fultz: Solvent effect on the heterogeneous adsorption and reaction of (2-chloroethyl)ethyl sulfide on nanocrystalline magnesium oxide. *Langmuir* **18**, 4819 (2002).
24. R. Richards, W. Li, S. Decker, C. Davidson, O. Koper, V. Zaikovski, A. Volodin, T. Rieker, and K.J. Klabunde: Consolidation of metal oxide nanocrystals. Reactive pellets with controllable pore structure that represent a new family of porous, inorganic materials. *J. Am. Chem. Soc.* **122**, 4921 (2000).
25. F. Mohandes, F. Davar, and M. Salavati-Niasari: Magnesium oxide nanocrystals via thermal decomposition of magnesium oxalate. *J. Phys. Chem. Solids* **71**, 1623 (2010).
26. M. Sharma and P. Jeevanandam: Synthesis of magnesium oxide particles with stacks of plates morphology. *J. Alloys Compd.* **509**, 7881 (2011).
27. T. Lopez, I. Garcia-Cruz, and R. Gomez: Synthesis of magnesium oxide by the sol-gel method: Effect of the pH on the surface hydroxylation. *J. Catal.* **127**, 75 (1991).
28. Y.X. Li and K.J. Klabunde: Nanoscale metal oxide particles as chemical regents. Destructive adsorption of a chemical simulant, dimethyl methyl phosophonate, on heat-treated magnesium oxide. *Langmuir* **7**, 1388 (1991).
29. J.V. Stark, D.G. Park, I. Lagadic, and K.J. Klabunde: Nanoscale metal oxide particles/clusters as chemical reagents. Unique surface chemistry on magnesium oxide as shown by enhanced adsorption of acid gases (sulfur dioxide and carbon dioxide) and pressure dependence. *Chem. Mater.* **8**, 1904 (1996).
30. G. Duan, X. Yang, J. Chen, G. Huang, L. Lu, and X. Wang: The catalytic effect of nanosized MgO on the decomposition of ammonium perchloride. *Powder Technol.* **172**, 27 (2007).
31. F. Chen, J. Zhao, and H. Hidaka: Highly selective deethylation of rhodamin B: Adsorption and photooxidation pathways of the dye on the TiO_2/SiO_2 composite photocatalyst. *Int. J. Photoenergy* **5**, 209 (2003).
32. Y. Hu, C. Li, F. Gu, and Y. Zhao: Facile flame synthesis and photoluminescent properties of core/shell TiO_2/SiO_2 nanoparticles. *J. Alloys Compd.* **432**, L5 (2007).
33. J. Fang, X. Bi, D. Si, Z. Jiang, and W. Huang: Spectroscopic studies of interfacial structures of CeO_2–TiO_2 mixed oxides. *Appl. Surf. Sci.* **253**, 8952 (2007).
34. D. Das, H.K. Mishra, K.M. Parida, and A.K. Dalai: Preparation, physicochemical characterization and catalytic activity of sulfated ZrO_2–TiO_2 mixed oxides. *J. Mol. Catal. A: Chem.* **189**, 271 (2002).
35. B. Pal, M. Sharon, and G. Nogami: Preparation and characterization of TiO_2/Fe_2O_3 binary mixed oxides and its photocatalytic properties. *Mater. Chem. Phys.* **59**, 254 (1999).
36. J. Lin and J.C. Yu: An investigation on photocatalytic activities of mixed TiO_2-rare earth oxides for the oxidation of acetone in air. *J. Photochem. Photobiol., A* **116**, 63 (1998).
37. J.R. Osman, J.A. Crayston, A. Pratt, and D.T. Richens: Sol-gel processing of IrO_2–TiO_2 mixed metal oxides based on an iridium acetate precursor. *J. Sol-Gel Sci. Technol.* **46**, 126 (2008).
38. Y.S. Jung, K.H. Kim, T.Y. Jang, Y. Tak, and S.H. Baeck: Enhancement of photocatalytic properties of Cr_2O_3-TiO_2 mixed oxides prepared by sol-gel method. *Curr. Appl. Phys.* **11**, 358 (2011).
39. S. Barison, S. Daolio, M. Fabrizio, and A.D. Battisti: Surface chemistry study of RuO_2/IrO_2/TiO_2 mixed-oxide electrodes. *Rapid Commun. Mass Spectrom.* **18**, 278 (2004).
40. B.M. Reddy, I. Ganesh, and A. Khan: Preparation and characterization of In_2O_3–TiO_2 and V_2O_5/In_2O_3–TiO_2 composite oxides for catalytic applications. *Appl. Catal., A* **248**, 169 (2003).
41. B. Julian-Lopez, M. Martos, N. Ulldemolins, J.A. Odriozola, E. Cordoncillo, and P. Escribano: Self-assembling of Er_2O_3–TiO_2 mixed oxide nanoplatelets by template-free solvothermal route. *Chem. Eur. J.* **15**, 12426 (2009).
42. J.R. Osman, J.A. Crayston, A. Pratt, and D.T. Ritcher: RuO_2–TiO_2 mixed oxides prepared by hydrolysis of metal alkoxides. *Mater. Chem. Phys.* **110**, 256 (2008).
43. L.R. Hou, C.Z. Yuan, and Y. Peng: Synthesis and photocatalytic property of SnO_2/TiO_2 nanotubes composite. *J. Hazard. Mater.* **139**, 310 (2007).
44. J. Bandara and U.W. Pradeep: Tuning of the flat-band potentials of nanocrystalline TiO_2 and SnO_2 particles with an outer-shell MgO layer. *Thin Solid Films* **517**, 952 (2008).
45. K.T. Ranjit, I. Martyanov, D. Demydov, S. Uma, S. Rodrigues, and K.J. Klabunde: A review of the chemical manipulation of nanomaterials using solvent: Gelation-dependent structures. *J. Sol-Gel Sci. Technol.* **40**, 335 (2006).
46. W. Wei, H. Li, S. Chen, C. Yuan, and Q. Yuan: One step synthesis of ZnO–MgO core-sheath structures. *Cryst. Res. Technol.* **44**, 861 (2009).
47. M.A. Aramendia, V. Borau, C. Jimenez, J.M. Marinas, A. Porras, and F.J. Urbano: Synthesis and characterization of MgO–B_2O_3 mixed oxides prepared by coprecipitation; selective dehydrogenation of propan-2-ol. *J. Mater. Chem.* **9**, 819 (1999).

48. B.M. Reddy, M.V. Kumar, and K.J. Ratnam: Selective oxidation of p-methoxytoluene p-methoxybenzaldehyde over V_2O_5/CaO–MgO catalysts. *Appl.Catal., A* **181**, 77 (1999).
49. S. Qiujie, L. Ning, and L. Yi: Preparation of MgO-supported Cu_2O catalyst and its catalytic properties for cyclohexanol dehydrogenation. *Chin. J. Catal.* **28**, 57 (2007).
50. M.E. Martin, R.M. Narske, and K.J. Klabunde: Mesoporous metal oxides formed by aggregation of nanocrystal. Behavior of aluminum oxide and mixtures with magnesium oxide in destructive adsorption of the chemical warfare surrogate 2-chloroethylethyl sulfide. *Microporous Mesoporous Mater.* **83**, 47 (2005).
51. M.B. Gawande, P.S. Branco, K. Parghi, J.J. Shrikhande, R.K. Pandey, C.A.A. Ghumman, N. Bundaleski, O.M.N.D. Teodoro, and R.V. Jayaram: Synthesis and characterization of versatile $MgO–ZrO_2$ mixed metal oxide nanoparticles and their applications. *Catal. Sci. Technol.* **1**, 1653 (2011).
52. E.V. Ilian, I.V. Mishakov, A.A. Vedyagin, A.F. Bedilo, and K.J. Klabunde: Synthesis of nanocrystalline VOx/MgO aerogel and their application for destructive adsorption of CF_2Cl_2. *NSTI-Nanotech.* **1**, 452 (2010).
53. H. Abimanyu, B.S. Ahn, C.S. Kim, and K.S. Yoo: Preparation and characterization of $MgO–CeO_2$ mixed oxide catalysts by modified coprecipitation using ionic liquids for dimethyl carbonate synthesis. *Ind. Eng. Chem. Res.* **46**, 7936 (2007).
54. M.E. Llanos, T. Lopez, and R. Gomez: Determination of surface homogeneity of $MgO–SiO_2$ sol-gel mixed oxides by means of CO_2 and ammonia thermodesorption. *Langmuir* **13**, 974 (1997).
55. C.L. Carnes, P.N. Kapoor, K.J. Klabunde, and J. Bonevich: Synthesis, characterization, and adsorption studies of nanocrystalline aluminum oxide and a bimetallic nanocrystalline aluminum oxide/magnesium oxide. *Chem. Mater.* **14**, 2922 (2002).
56. H. Sieger, J. Suffner, H. Hahn, A.R. Raju, and G. Miehe: Thermal stability of nanocrystalline Sm_2O_3 and Sm_2O_3-MgO. *J. Am. Ceram. Soc.* **89**, 979 (2006).
57. M.A. Aramendia, V. Borau, C. Jimenez, A. Marinas, J.M. Marinas, J.A. Navio, J.R. Ruiz, and F.J. Urbano: Synthesis and textural-structural characterization of magnesia, magnesia-titania, and magnesia-zirconia catalysts. *Colloids Surf., A* **234**, 17 (2004).
58. H.S. Jung, J.K. Lee, M. Nastasi, S.W. Lee, J.Y. Kim, J.S. Park, K.S. Hong, and H. Shin: Preparation of nanoporous MgO-coated TiO_2 nanoparticles and their application to the electrode of dye-sensitized solar cells. *Langmuir* **21**, 10332 (2005).
59. N. Stubicar, A. Tonejc, and M. Stubicar: Microstructural evolution of some $MgO–TiO_2$ and $MgO–Al_2O_3$ powder mixtures during high-energy ball milling and post-annealing studied by x-ray diffraction. *Alloys Compd.* **370**, 296 (2004).
60. D. Osabe, H. Seyama, and K. Maki: Evaluation of crystallinity in TiO_2 films with mixed structures grown on MgO (001) substrates by argon-ion beam sputtering based on infrared reflection-absorption spectra. *Appl. Opt.* **41**, 739 (2001).
61. J. Bernard, F. Belnou, D. Houidvet, and J.M. Haussonne: Synthesis of pure $MgTiO_3$ by optimizing mixing/grinding condition of MgO + TiO_2 powders. *J. Mater. Process. Technol.* **199**, 150 (2008).
62. T. Lopez, J. Hernandez, R. Gomez, X. Bokhimi, J.L. Boldu, E. Munoz, O. Novaro, and A. Garcia-Ruiz: Synthesis and characterization of $TiO_2–MgO$ mixed oxides prepared by the sol-gel method. *Langmuir* **15**, 5689 (1999).
63. J. Bandara, C.C. Hadapangoda, and W.G. Jayasekera: TiO_2/MgO composite photocatalyst: The role of MgO in photoinduced charge carrier separation. *Appl. Catal., B* **50**, 83 (2004).
64. Z. Wen, X. Yu, S.T. Tu, J. Yan, and E. Dahlquist: Biodiesel production from waste cooking oil catalyzed by $TiO_2–MgO$ mixed oxides. *Bioresour. Technol.* **101**, 9570 (2010).
65. T. Lopez, J. Hernandez-Ventura, D.H. Aguilar, and P. Quintana: Thermal phase stability and catalytic properties of nanostructured TiO_2-MgO sol-gel mixed oxides. *J. Nanosci. Nanotechnol.* **8**, 6608 (2008).
66. S. Utamapanya, K.J. Klabunde, and J.R. Schlup: Nanoscale metal oxide particles/clusters as chemical reagents. Synthesis and properties of ultrahigh surface area magnesium hydroxide and magnesium oxide. *Chem. Mater.* **3**, 175 (1991).
67. H.K. Kammler, L. Mädler, and S.E. Pratsinis: Flame synthesis of nanoparticles. *Chem. Eng. Technol.* **24**, 583 (2001).
68. G.W. Jones, B. Lewis, and H. Seaman: The flame temperature of methane-oxygen, methane-hydrogen and methane-acetylene with air. *J. Am. Chem. Soc.* **53**, 3992 (1931).
69. D. Urzica and E. Gutheil: Structure of laminar methane/nitrogen/oxygen, methane/oxygen and methane/liquid oxygen counterflow flames for cryogenic conditions and elevated pressures. *Z. Phys. Chem.* **223**, 651, (2009).
70. H.J. Fissan: Temperature distribution in open oxygen air methane-oxygen flame. *Combust. Flame* **17**, 355 (1971).
71. K.M. Shrestha, C.M. Sorensen, and K.J. Klabunde: Synthesis of CuO nanorods, reduction of CuO into Cu nanorods, and diffuse reflectance measurements of CuO and Cu nanomaterials at near infrared region. *J. Phys. Chem. C* **114**, 14368 (2010).
72. A.W. Czanderna, C.N.R. Rao, and J.M. Honig: The anatase-rutile transition part 1.— Kinetics of the transformation of pure anatase. *Trans. Faraday Soc.* **54**, 1069 (1958)
73. J.S.J. Hargreaves, G.J. Hutchings, R.W. Joyner, and C.J. Kiely: The relationship between catalysts morphology and performance in oxidative coupling of methane. *J. Catal.* **135**, 576 (1992).
74. M. Che and A.J. Tench: Characterization and reactivity of molecular oxygen species on oxide surfaces. *Adv. Catal.* **32**, 1 (1983).
75. L. Zhang, H. Ji, Y. Lei, and W. Xiao: Oxygen adsorption on anatase surfaces and edges. *Appl. Surf. Sci.* **257**, 8402 (2011).
76. M. Anpo, Y. Yamada, and Y. Kubokawa: Photoluminescence and photocatalytic activity of MgO powders with coordinatively unsaturated surface ions. *J. Chem. Soc. Commun.* **50**, 714 (1986).
77. G. Pacchioni and A.M. Ferrari: Surface reactivity of MgO oxygen vacancies. *Catal. Today* **50**, 533(1999).
78. W.R. Smith and D.G. Ford: Adsorption studies on heterogeneous titania and homogeneous carbon surfaces. *J. Phys. Chem.* **69**, 3587 (1965).
79. Z. Ding, G.Q. Lu, and P.F. Greenfield: Role of the crystallite phase of TiO_2 in heterogeneous photocatalysis for phenol oxidation in water. *J. Phys. Chem. B* **104**, 4815 (2000).

Supplementary Material

Supplementary material can be viewed in this issue of the *Journal of Materials Research* by visiting http://journals.cambridge.org/jmr.